RSC Advances

PAPER

View Article Online
View Journal | View Issue

Cite this: *RSC Adv.*, 2021, **11**, 20109

An XPS study of HCN-derived films on pyrite surfaces: a prebiotic chemistry standpoint towards the development of protective coatings

Cristina Pérez-Fernández, Marta Ruiz-Bermejo, Santos Gálvez-Martínez and Eva Mateo-Martí *

Traditionally, the effect of mineral surfaces on increasing molecular complexity has been considered a major issue in studies about the origin of life. In contrast, herein, the effects of organic films derived from cyanide over an important prebiotic mineral, pyrite, are considered. An XPS spectroscopy study was carried out to understand the surface chemistry of the HCN-derived polymer/pyrite system. As a result, the simulation of a plausible prebiotic alkaline hydrothermal environment led to the identification of an NH_4CN-based film with protective corrosion properties that immediately prevented the oxidation of the highly reactive pyrite surface. In addition, the effect of coating with antioxidant properties was preserved over a relatively long time, and the polymeric film was very stable under ambient conditions. These results increase the great potential of HCN polymers for development as a cheap and easily produced new class of multifunctional polymeric materials that also show promising and attractive insights into prebiotic chemistry.

Received 5th April 2021
Accepted 12th May 2021

DOI: 10.1039/d1ra02658e

rsc.li/rsc-advances

Introduction

HCN is a ubiquitous molecule in the Universe that polymerises easily under a wide variety of experimental conditions. Additionally, HCN polymers belong to a heterogeneous family of coloured solids ranging from yellow and orange-brown to black, depending on the grade of polymerisation and/or cross-linking. These fascinating substances are widely known in the fields of prebiotic chemistry and astrobiology.[1,2] Recently, computational studies have pointed out the important role of HCN water chemistry in primeval abiotic synthesis of RNA and protein precursors,[3] and geological reports have provided new insights to consider the relatively high concentrations of cyanide in different aqueous alkaline environments of the early Earth.[4] HCN can polymerise only above a concentration of 0.01 M because below this concentration, the hydrolysis processes are dominant.[5] In addition to the key role of HCN polymers in studies on the origin of life,[6] these organics have been revealed as promising materials,[7] especially as coatings with potential applications in biomedicine, stormwater/greywater filtration[8–13] and more recently as protective films with antioxidant activity.[14] Moreover, they have been considered for the design of polymeric materials with emerging properties such as semiconduction, ferroelectricity, photocatalytic activity or capacitance.[15–18] The possibilities of HCN polymers in the development of a new generation of multifunctional materials have also extended and modified their role in astrobiological research beyond the traditional viewpoint that they are simple precursors to biomonomers,[1] expanding the field of prebiotic chemistry.[15,19] Moreover, it is well known that the synthetic conditions allow tuning of the structural characteristics and extension of the properties of HCN polymers.[15,20–22]

Mineral surfaces could potentially have allowed for almost any type of general catalysis, with low specificity and efficiency, in several prebiotic environments. Among these mineral surfaces, pyrite (FeS_2) is crucial for explaining the iron–sulfur world hypothesis about the origin of a possible proto-metabolism.[23] In addition, many chemical, geochemical and biological reactions occur at pyrite surfaces.[24] Oxidation studies have shown that pyrite is a very reactive surface under ambient conditions, oxidising rapidly in air and forming iron oxide and ferric sulfate species.[25,26] Other possible oxidation products include Fe-hydroxide or Fe-oxyhydroxide, monosulfide, disulfide and polysulfide depending on the conditions and duration of the oxidation processes. Furthermore, recent studies conclude that UV photocatalysis on pyrite surfaces may have been a natural mechanism of prebiotic fixation of nitrogen into ammonium sulfate, which is then easily released from the surface upon contact with liquid water.[27] The reactivity of pyrite in aqueous solutions is determined by the ability of the first oxidized layer to adsorb certain molecules, passivating the surface and preventing further oxidation.

Therefore, due to the great ability of HCN and its derivatives, such as KCN, NH_4CN and aminomalononitrile or

Centro de Astrobiología (INTA-CSIC), Dpto. Evolución Molecular, Ctra. Torrejón-Ajalvir, km 4, Torrejón de Ardoz, 28850 Madrid, Spain. E-mail: mateome@cab.inta-csic.es

diaminomalononitrile (AMN and DAMN, the formal trimer and tetramer, respectively, of HCN), to produce brown organic films over a wide diversity of substrates[8] and the plausible convergence between HCN and pyrite in an aqueous prebiotic scenario, several studies were carried out to explore the interaction between HCN on a pyrite surface in a plausible alkaline prebiotic environment. These alkaline environments are considered good places for the increase in molecular complexity and eventually for the emergence of life.[3,4,28,29] It is also well known that the polymerization of HCN in water is only driven under alkaline pH conditions (from 8 to 10)[30] (pK_a of HCN 9.2), which makes HCN polymerization practically equivalent to cyanide polymerization. Based on these particular considerations, herein, we studied the interaction between NH_4CN-derived coatings on a pyrite surface. Thus, pyrite samples were directly immersed in aqueous solutions of NH_4CN under different reaction conditions using an inert atmosphere of N_2 simulating prebiotic conditions or under atmospheric air conditions as a control experiment. The pristine pyrite surface (coating-free) and the coated pyrite surfaces were comprehensively studied by X-ray photoemission spectroscopy (XPS) to fully characterise not only the surface chemistry of the pyrite but also the changes undergone by the polymeric films after exposure to ambient conditions of air, moisture and light.

The scarce previous reports about the mineral–HCN interactions were focused on the effect of the mineral, mainly montmorillonite clays, on the oligomerization/polymerization processes of HCN,[31–33] or on the mechanism of concentration of HCN.[34,35] Herein, by contrast, the focus is on the effect of the polymeric films on the mineral surfaces, which were analysed. Thus, when the pyrite surfaces were immersed in NH_4CN solutions, they were coated and immediately protected against the oxidation by water. This protective effect against ambient oxidation conditions was maintained almost inalterably over the time considered herein. This study shows that fundamental research in prebiotic chemistry can lead to the development of useful, inexpensive and easily produced organic polymeric materials that can be used, in this particular case, as efficient protective corrosion coatings and it can also provide insight into the puzzling questions about the origin of life, providing new insights into organic–mineral interactions.

Results

Comparative study of pyrite surfaces exposed to pure water and aqueous NH_4CN solutions

To evaluate the coating properties of NH_4CN-based films on pyrite surfaces, we compared clean pyrite surfaces, clean "coating-free" pyrite surfaces immersed in water solutions (at 80 °C for 40 min under anoxic conditions), and clean pyrite surfaces immersed in aqueous NH_4CN solutions under anoxic and air conditions (at 80 °C for 40 min). The temperature and reaction time were chosen based on previous kinetic studies,[20,36] to create effective coatings but to prevent significant production of insoluble NH_4CN polymers. Additionally, oxygen from the air has an active role in the production of cyanide polymers and subsequently on their respective properties.[37] In addition, anoxic conditions are necessary to simulate prebiotic chemistry conditions.

Fig. 1a shows a comparison of the XPS spectra for the iron (Fe 2p core level) in the four different cases studied herein. Clean pyrite (black line) and coated pyrite surfaces under anoxic conditions (blue line) have similar spectral shapes. However, it is remarkable that after only 40 min of water immersion (dashed black line), intense bands at 710.8 and 712.9 eV appear in the spectrum of the coating-free pyrite. These bands are assigned to the iron oxide (Fe_2O_3) and FeOOH species. However, the iron spectra for the coated pyrite surface under air conditions (red line) show a lower intensity of the Fe 2p signal than the other cases, meaning that the adsorption layer of the NH_4CN-based coatings on the pyrite surface is thicker than the

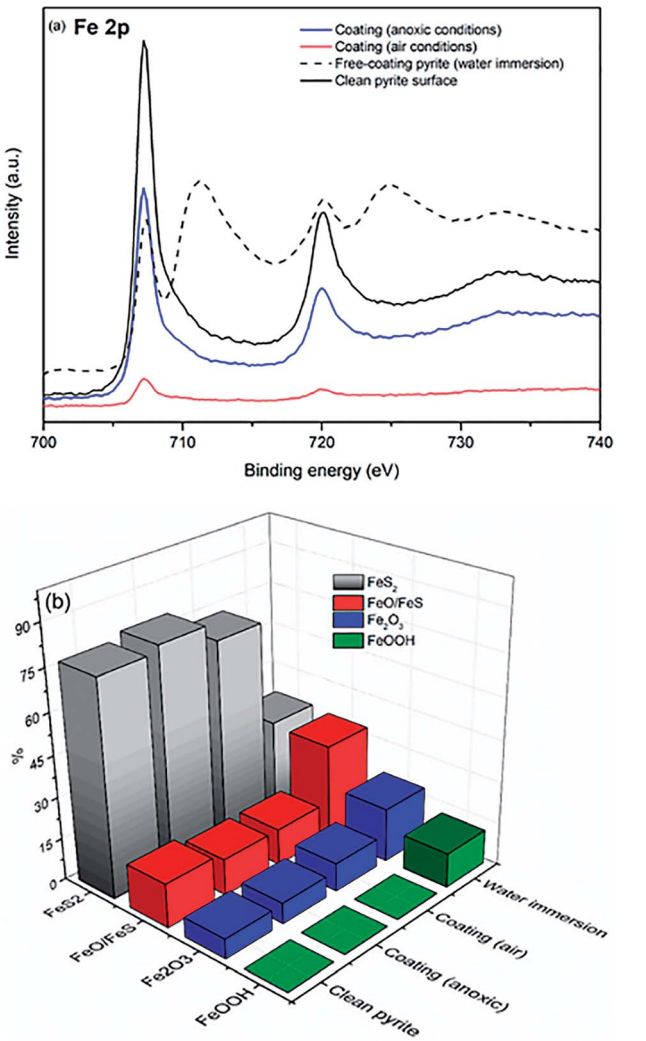

Fig. 1 (a) XPS photoemission spectra of the Fe 2p core level for the pyrite surfaces: a clean pyrite surface (solid black line), coating-free pyrite immersed in water (80 °C, 40 min, dashed black line) and coated pyrite surfaces with NH_4CN-based films synthesised under anoxic (solid blue line) and air conditions (solid red line); (b) comparative percentages of Fe species in coating-free pyrite surfaces and pyrite surfaces with NH_4CN-based coatings.

one adsorbed under anoxic conditions, as the iron surface signal in the XPS spectra has greater attenuation. Pyrite surfaces immersed in aqueous NH_4CN solutions under anoxic and air conditions have the capability to avoid the appearance of iron oxide and oxyhydroxide species on the surface, meaning that the formation of a coating layer under the tested experimental conditions and the capability to nicely protect the surfaces were successful.

Fig. 1b shows a bar diagram for the percentage of the iron chemical species present in each of the four pyrite surface cases studied described above. It is seen that coating-free pyrite immersed in water presents remarkable degradation of the FeS_2 surface into oxidized iron (4% FeS + FeO and 39% Fe_2O_3) and FeOOH (25%) species, whereas after being immersed in the NH_4CN solutions, the pyrite surface shows the absence of FeOOH species and a small amount of oxide iron species (17% FeO + FeS and 10% Fe_2O_3 for air conditions and 13% FeO + FeS and 7% Fe_2O_3 for anoxic conditions); the percentages are similar to those of the clean pyrite surface (19% FeO + FeS and 8% Fe_2O_3). These chemical species percentages are in good agreement with the sulfur XPS results (data not shown), whereas two components are described for all cases: the main component at ~162.7 eV is assigned to the FeS_2 species, and the second component at ~164.9 eV is related to polysulfide species. Therefore, the NH_4CN solution formed a protective film coating on the pyrite surface faster than the water solution and could activate the formation of oxidised species on the pyrite surface. A short coating formation time (40 min) is critical for avoiding the presence of pyrite degradation species on the surface. Thus, an effective film coating rapidly formed before the appearance of oxidised species on the surface.

Furthermore, the two pyrite surfaces with NH_4CN-based coatings present similar chemical species percentages to the clean pyrite surfaces that have not been immersed in water solution.

Characterization of the NH_4CN-based coatings under anoxic and air synthetic conditions

It has been demonstrated that the properties of HCN-derived polymer coatings are dependent on several factors, *e.g.*, the thickness of the coating films is directly related to the reaction time.[13,14] Furthermore, the morphology of the AMN-based polymer coatings appears to be influenced by the substrate material and by the concentration of buffer used.[7] However, no study has been carried out to show the role played by oxygen in the production of these polymeric HCN-derived coatings. As shown above (Fig. 1a), the presence of oxygen during polymer adsorption drastically diminished the XPS intensity from the Fe 2p signal. Thus, a detailed comparison study between NH_4CN-based films produced under anoxic and air conditions was performed in order to understand the coating properties, which were likely different. The mechanism of different synthesis conditions and their influence on the polymeric layer formation by coating the pyrite surface were studied.

The XPS analysis of the pyrite surfaces after immersion in NH_4CN solutions under both anoxic and air conditions revealed the presence of carbon, oxygen and nitrogen (see Fig. 2), proving the successful formation of the coating layer on the surface, with the nitrogen feature being the fingerprint of the polymer on the pyrite.

In the case of polymeric film formation under inert conditions, the best-fit curve for the C 1s peak was achieved using three components. The first carbon component had a binding energy (B.E.) of 285.3 eV and was attributed to the C–H and C–C groups, the second component at 286.9 eV corresponded to C–S, C–N and C–O groups, whereas the third component was observed at 288.8 eV, which can be assigned to COOH or COO^- groups. This assignment of the C 1s components shows some similarities to analogous AMN-based films.[7] Nevertheless, some differences can be pointed out, as the C 1s peak was fitted using five components instead of three, and its shape was clearly different from that of the peak shown in Fig. 2a. This comparison is also in agreement with the fact that the initial monomer used to produce HCN-derived polymers leads to the production of polymeric materials with different structural properties.[15] The O 1s peak shows three different contributions. The first at 531.7 eV corresponds to C=O and atmospheric air, the second component at 533.2 eV is assigned to the COOH and OH groups, and the third component at 534.9 eV is related to the atmospheric water and charging effect from the sample, as previously reported.[38] The best-fit curve of the N 1s peak consists of three components: the first component at 399.2 eV corresponds to the N–C, N–H and –C=N groups; the second component at 400.0 eV corresponds to NH_2; and the last component corresponds to NH_3^+ groups or ammonium salt at 402.7 eV.

In the case of polymeric film formation under air conditions, similar components are observed for the C 1s, O 1s and N 1s

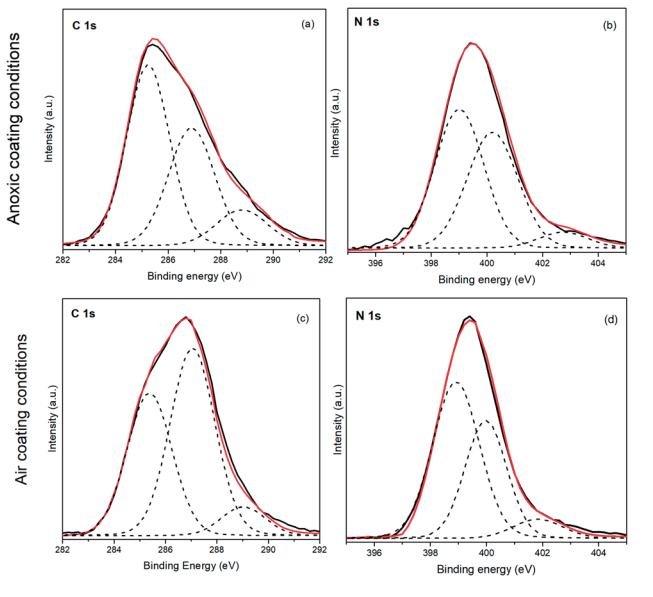

Fig. 2 XPS photoemission spectra of the C 1s and N 1s core level peaks of the NH_4CN-based films synthesised under anoxic (a and b) and air conditions (c and d) on a pyrite surface (measured immediately after the coating). Experimental core-level spectra (black), the result of a fitting of several components (red) and components (black dotted line).

peaks. A comparison between the two conditions did not show remarkable differences for the nitrogen components or for the composition percentages (Fig. 2 and Table 1). However, for carbon species, a slight increase in the C–N, C–O and C–S components at 287.1 eV is observed under air coating conditions with respect to the one performed under anoxic coating conditions. Therefore, this evidence indicates that the polymers would be more functionalised than the ones produced under inert conditions. However, the main component of carbon is related to the C–C and C–H functionalities (hydrocarbon chains) in the presence of air conditions. The main difference in the oxygen region is an increase in the component at 534.3 eV, which is assigned to the charge effect under air conditions. This increase could be related to the greater thickness of the layer adsorbed on the pyrite surface, which could increase that charging effect.

Therefore, as the main difference between both synthesis conditions seems to be related to the thickness of the polymeric films on the pyrite surface, we calculated the following values for both conditions. In the case of air conditions, the N/Fe ratio is 58.7, whereas for the anoxic conditions coating, this ratio is 3.8. In addition, the thickness of the polymer layer under anoxic conditions was 15 Å, whereas that under air conditions was 65 Å; this coating was five times thicker than the other one. These calculations are in good agreement with the results shown in Fig. 1a with respect to the attenuation of the Fe 2p signal and with the N/Fe ratios found for both coatings. Moreover, the presence of air during the formation of the cyanide-based coatings has a significant influence on the structure of the protective film, as reflected in the N/C relationships found for both polymeric films. The N/C ratio was 0.54 under air conditions, and the N/C ratio was 0.32 for the NH_4CN-based film formed under anoxic conditions. In summary, the presence of air during the formation process of the NH_4CN-based films has a significant influence both in the structural characteristics of the film and in its respective thickness of the polymer layer, which is five times thicker when synthesised in air conditions.

Fig. 3 shows a comparison of both polymeric films over the same reaction time (40 min) on pyrite surfaces under inert and air conditions. An increase in the XPS nitrogen signal (signature from the HCN-derived polymers) and the attenuation of the Fe 2p and S 2p (signals from the substrate) are observed in the case of the NH_4CN-based film coating synthesised under air conditions, as expected from the above explanation. This evidence seems to prove a higher polymerization conversion, meaning a thicker coating layer production on the pyrite in the case of NH_4CN-based film coating synthesised under air conditions, indicating that the presence of oxygen during the covering stage is a significant factor. A comparison of the different polymeric deposition conditions shows remarkable differences in surface coating layer formation.

Once successful NH_4CN-based film formation on the pyrite surfaces was verified under both anoxic and air coating conditions and their differences were identified, a comparison of the effectiveness of the coating properties against surface degradation due to ambient exposure over time was performed.

Table 1 A comparison study of C 1s, O 1s and N 1s core-level peaks, deconvolution and ratios of their component peaks of the HCN/pyrite surface under inert and air atmosphere conditions

Elements	Assignments	B.E. (eV)	% (anoxic)	B.E. (eV)	% (air)
C	C–H, C–C	285.3	52	285.4	40
	C–S, C–N, C–O	286.9	36	287.1	52
	COOH, COO^-	288.8	12	289.1	8
O	Air, C=O	531.7	37	531.5	33
	COOH, OH	533.2	39	532.8	28
	Charge effect	534.9	24	534.3	39
N	N–C, N–H, C=N	399.2	52	398.9	56
	NH_2	400.0	42	400.0	37
	NH_3^+ ammonium salt	402.7	6	401.9	7

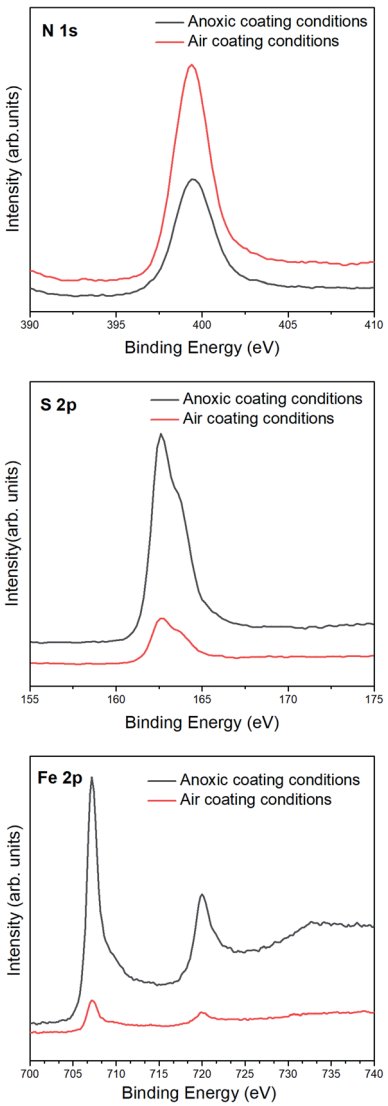

Fig. 3 XPS photoemission spectra of the N 1s, S 2p and Fe 2p core level peaks of pyrite surfaces coated by NH_4CN-based films synthesised under anoxic (black line) or air conditions (red line).

Chemical evolution of the pyrite surface coated by NH_4CN-based films exposed to ambient conditions

A comparison study was performed to explore the evolution of the pyrite–organic coating system after exposure to ambient conditions for 40 days. Chemical changes on the surface were measured by XPS. Fig. 4 shows the time evolution of the Fe species from each pyrite case studied (free polymer, polymer coating in air and inert conditions) over time (0 and 40 days).

Fig. 4 shows that the number of FeS_2 species drastically decreased for the coating-free pyrite surface after exposure to ambient conditions for 40 days, with slight decreases in the film formed under anoxic conditions; however, in the film formed under air conditions, the quantity of FeS_2 species remained similar to that at 0 days. Fe(III) oxide species (Fe_2O_3) and iron sulfates were the predominant species on the coating-free surface. However, for surfaces covered with polymeric coatings, the Fe(III) oxide species (Fe_2O_3) remained practically constant in both cases and was significantly lower than for the coating-free surface. Finally, sulfate species appeared on the surface after 40 days of exposure to ambient conditions. A higher conversion to sulfate species ($FeSO_4$) was observed after 40 days of exposure to ambient conditions in the case of coating-free pyrite, whereas in the presence of the NH_4CN-based coatings, the formation of sulfate species was highly reduced, and the lowest quantity of sulfates was detected for the NH_4CN-based film produced under anoxic conditions. Therefore, significant degradation of the pyrite surface was observed in the absence of the polymeric film, which plays a crucial surface protection role.

Consequently, the chemical species evolution and the appearance of different percentages of sulfur and iron species on the surface prove that NH_4CN-based films provide protective properties to the pyrite surfaces. Furthermore, the polymeric film synthesised using anoxic conditions offers the highest surface protection from the cases studied. In addition, even if the film produced under anoxic conditions is thinner than the film synthesised under air conditions, the coating properties for the pyrite surface are greater. This increase in the protective effect may be related to the different chemical compositions of the films, as shown above by the N/C ratios. Again, it is proven that the synthetic conditions have an influential role in the properties of HCN-derived polymers.

Therefore, NH_4CN-based films act as surface coatings, protecting the pyrite surfaces from air, moisture and light oxidation processes under ambient conditions. Furthermore, XPS results confirm that pyrite is less oxidized when it is coated with the NH_4CN-based film produced under plausible prebiotic conditions, since this coating better protects the surface and is more efficient than the one synthesised under air conditions, even with thicker film formation on the surface.

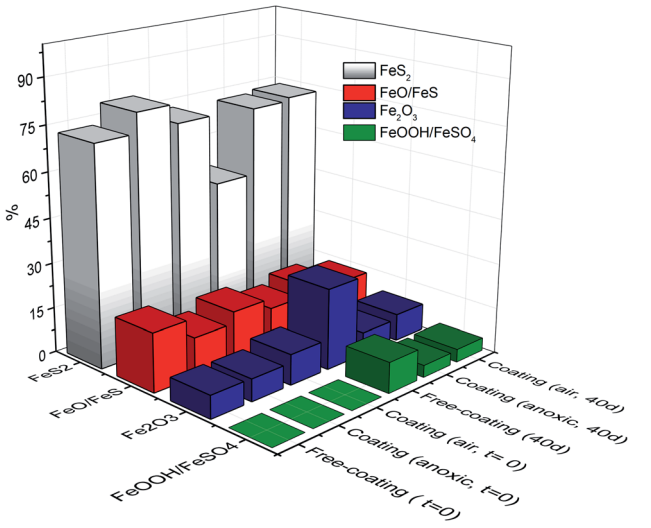

Fig. 4 Time evolution of the Fe species on the coating-free pyrite surface and from NH_4CN-based films under anoxic and air conditions at 0 and 40 days of ambient exposure.

Chemical evolution of a pyrite–NH_4CN film system produced under plausible prebiotic conditions exposed to a current Earth environment

After analysing the results of the previous section, a detailed study of the pyrite surface coated by the NH_4CN-based film produced under anoxic conditions was performed at different times to understand the properties and stability of a thin coating layer exposed to ambient conditions over time. This study is relevant to prebiotic chemistry because if the coatings are resistant to and highly protective against the current oxidizing conditions of the modern Earth, they should be even more effective under the reductive/neutral conditions of the early Earth. It is true that in the present case, the effect of the higher UV radiation of the primitive Earth is not considered, but other works are in progress to determine this effect. Thus, XPS measurements were taken at 0, 7, 40 and 60 days for the pyrite surface coating with the NH_4CN-derived film synthesised under anoxic conditions. The ambient conditions are referenced to the temperature, pressure, moisture and light of a conventional laboratory.

Fig. 5 shows an XPS comparison of the N, S and Fe spectra of clean pyrite surfaces (coating-free analysed at zero time) and the pyrite surface coated by NH_4CN-based films under inert conditions, measured immediately after coating at zero time and after 7, 40 and 60 days of ambient condition exposure, which helps to elucidate in detail the coating properties and pyrite surface evolution after exposure to ambient conditions.

Nitrogen is the fingerprint of the successful NH_4CN-based film coating formation on the pyrite surface. Therefore, for the spectrum of coating-free pyrite, there is practically no signal (Fig. 5a); then, when the pyrite surface is coated (zero time), the nitrogen signal is highly noticeable. A detailed deconvolution of the N 1s peak shows three components, as discussed above. The most intense nitrogen XPS signal corresponds to the first measure immediately after coating (meaning zero time), and then as time evolves from 0 to 60 days, the intensity from the nitrogen signal decreases (Fig. 5a). This decrease in the intensity of the characteristic nitrogen signal due to atmospheric exposure could be related to atmospheric species adsorption on top of the polymeric layer (attenuating the characteristic nitrogen signal) since the shape and relative intensity of the components of the N 1s peak are not dramatically changed

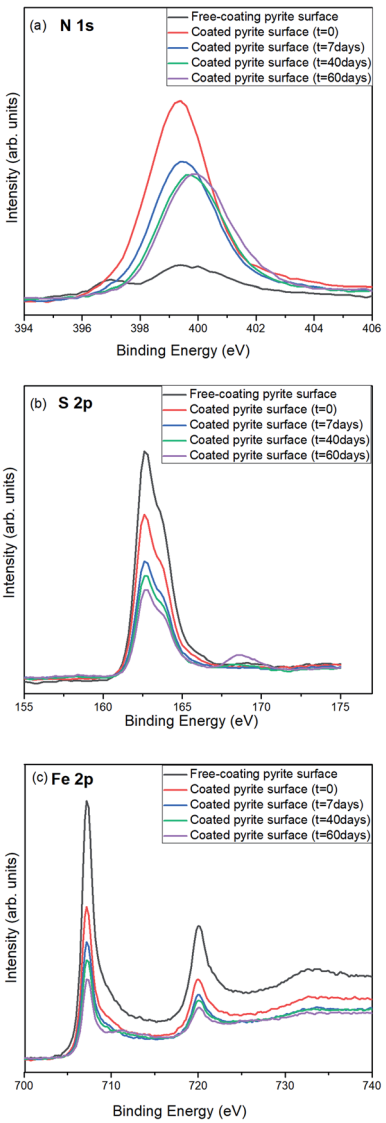

Fig. 5 XPS photoemission spectra of N 1s, S 2p and Fe 2p on the clean pyrite surface (coating-free analysed at zero time, immediately after cleaning procedure (black line)), the pyrite surface coated by the NH_4CN-based film under inert conditions, measured immediately after coating (solid red line) and the pyrite surface coated by the NH_4CN-based film, measured after 7 (blue line), 40 (green line) and 60 days (purple line) of exposure to ambient conditions.

during the interval of time considered here (0–60 days). It seems that no chemical degradation processes are affected by the polymeric coating, and only an attenuation of the signal is observed over time (Table 2 and Fig. 5a). Therefore, this plausible prebiotic polymeric coating seems certainly resistant to the current oxidising ambient conditions.

The sulfur XPS spectra (Fig. 5b) show that once the pyrite surface is coated, the sulfur intensity signal decreases due to the presence of the polymeric layer on the pyrite surface. At short times (0 and 7 days), the surface composition does not change (see Table 2), as the signal corresponds to FeS_2 at 162.6 eV and a second component at 164.5 eV corresponds to polysulfides. XPS measurements performed at 40 and 60 days show the

Table 2 A comparison of N 1s, S 2p and Fe 2p core-level peaks, deconvolution and ratios of their component peaks of the HCN/pyrite surface exposed for different times (0, 7, 40 and 60 days) under air atmosphere conditions

Assignments		Binding energies (eV)	Coating-free	Time (days) 0	7	40	60
% N	N–H/N–C/N=C	~399	—	52	52	52	51
	NH_2	~400	—	42	43	45	42
	NH_3^+	~402	—	6	5	4	6
S	FeS_2	~162	89	90	90	83	73
	Polysulfides	~164	11	10	10	10	10
	$FeSO_4$	~168	—	—	—	7	17
Fe	FeS_2	~707	77	80	81	72	71
	FeO/FeS	~709	18	13	13	16	11
	Fe_2O_3/FeOOH	~711	5	7	6	8	13
	$FeSO_4$	~713	—	—	—	4	5

appearance of a new third component at 168.8 eV, which corresponds to the presence of a new species, iron sulfate, on the pyrite surface. Remarkably, the exposure of the coating-free pyrite surface to ambient conditions leads to a high formation of sulfates after 40 and 60 days of exposure (7 and 17%, respectively, see Fig. 5).

Finally, in the case of iron species, the surface composition of clean pyrite shows a main peak at 707.5 eV corresponding to FeS_2, a second peak at 709.2 eV for FeS and FeO species; additionally, a third peak at 711.3 eV is assigned to FeOOH and Fe_2O_3 species; signals for similar species appear and their percentages are shown after the surface is exposed to air conditions for 7 days (Table 2). For the XPS measurements performed at longer exposure times of 40 and 60 days, the appearance of a fourth component at 713.5 eV, which is assigned to the iron sulfate species, is remarkable and is in good agreement with the data for the sulfur species; consequently, only highly oxidised species are observed after longer exposure times (40 and 60 days).

Therefore, the polymeric NH_4CN-based film synthesised under anoxic conditions seems to be highly stable under ambient conditions, and air, moisture and light also protect the pyrite surface against oxidation relatively well. The coated pyrite surface might be affected by corrosion after longer exposure times due to the morphology of the polymeric protected layer and/or the thinness of the coating film. In any case, for the first time, the good stability of a plausible prebiotic NH_4CN-based coating under ambient conditions was demonstrated.

As a quantitative summary of the results explained above, the presence of NH_4CN-based film coatings on pyrite surfaces prevented the formation of iron sulfate species for at least 7 days; for longer exposure times, the appearance of iron sulfate species was reduced by more than 50%. Furthermore, iron oxides (Fe_2O_3) were highly reduced from 26.7% to 8.9% for air synthesis coating conditions, and for the most successful coating formed in inert synthesis conditions up to 7.4%, even after 60 days, the percentage was reduced by 50% (Table 3).

Table 3 Quantitative summary of the surface oxidative degradation compounds and atmospheric exposure times of a coating-free pyrite surface and pyrite surfaces coated by NH_4CN-derived films obtained under air conditions or under an inert atmosphere of nitrogen

				NH_4CN-based film coatings					
	Coating-free surface			Air synthetic conditions		Anoxic synthetic conditions			
Time (days)	0	7	40	0	40	0	7	40	60
Fe_2O_3	7.6%	8.7%	26.7%	10.1%	8.9%	7.4%	6.0%	7.4%	13.8%
Iron sulfates	—	6.3%	10.2%	—	4.3%	—	—	4.0%	4.0%

Discussion and outlook

In the only preliminary work about the antioxidant properties of HCN-derived coatings, it was shown that AMN-based films have electrochemical moieties that present antioxidant properties; these were measured by the quenching of 2,2-diphenyl-1-picrylhydrazyl (DPPH).[14] In this previous study, the increase in the thickness of the films and their antioxidant activity with the deposition time as well as the morphologic modifications suffered by the coatings were discussed in terms of the deposition time. Better antioxidant activity was found for AMN-based films with an ~30 nm thickness using a deposition time of 25–30 h under atmospheric and ambient temperature conditions. Herein, it was demonstrated that the simulation of plausible prebiotic conditions led to the generation of a film thinner than previously reported but also with high potential as an antioxidant protective agent. This plausible prebiotic NH_4CN-based film prepared under hydrothermal alkaline conditions could protect against oxidation even on a highly reactive surface such as pyrite. In addition, the antioxidant properties of coatings are preserved over a relatively long time, and the polymeric film is truly stable under ambient conditions, which eventually led us to think that under reductive/neutral conditions of a prebiotic atmosphere, the protective effect would be positive for a longer period of time. In this way, not only the effect of minerals on organic reactions but also the effect of organics on mineral surfaces must be kept in mind in experiments on the increase in molecular complexity in prebiotic scenarios, as was not considered until now. In this particular case, pyrite was protected against oxidation and the superficial catalytic and redox properties of this mineral were inhibited or avoided, since these properties are directly related to the oxidising species on the FeS_2 surface. However, the presence of a highly stable prebiotic coating opens new perspectives to explore from the point of view of prebiotic chemistry since this type of film could be functionalised through the amine ($-NH_2$) and carboxylate ($-COO^-$) groups, leading to even more potential prebiotic reactions to be explored using HCN as the main molecule. Additionally, the photocatalytic activity of HCN-derived polymers and other related compounds encourages research on the photostability and photoactivity of this new generation of organic films. Additionally, in the same way that different minerals can cause different effects in the oligomerisation/polymerisation of HCN, as discussed above, and the morphology of the HCN-derived films depends on the substrate,[7] the interaction of the cyanide solutions with different minerals might lead to different effects than those reported here due to the distinguishing nature of the mineral surface. These aspects will be studied in future works.

Returning to the corrosion protection of the NH_4CN-based films on the pyrite surfaces, these coatings may offer possibilities to develop new multifunctional materials, as was indicated. Deterioration of material when it interacts with its environment is a global problem. Among the different strategies employed to avoid corrosion, the use of coatings and corrosion inhibitors are the most popular. The current environmental and economic challenges encourage the development of materials that must be easily obtained using low-cost and green chemistry processes. In this context, the prebiotic coatings presented herein may be considered good examples. Importantly, HCN-based coatings can be deposited on several substrates under different reaction conditions, which modifies the surface chemistry, controlling their physicochemical properties. For example, deep analysis shows that for the pyrite surface coated by the NH_4CN-based film produced under air conditions, the N/C ratio was 0.54, which is sufficiently similar to that found for the combined glass/KCN-based film, $N/C = 0.645 \pm 0.003$, and to those of the glass and polystyrene/AMN-based composite films, 0.57 ± 0.02 and 0.61 ± 0.02, respectively.[8,21] In contrast, the N/C ratio was 0.32 for the NH_4CN-based film formed herein under anoxic conditions. These results seem to indicate that air conditions lead to the production of coatings with richer composition in nitrogen with respect to prebiotic conditions of synthesis, but the anoxic reaction conditions seem to produce coatings that are more effective against corrosion. The different N/C ratios and behaviours of our NH_4CN-based coatings seem to indicate structural variations in their polymeric networks. This hypothesis will be studied in depth to develop HCN-derived coatings with applications related to the use of a variety of materials to shield the interior and exterior of important structures and to protect treated substrates from weather, UV radiation, and corrosion from marine biofouling.

Conclusions

The simulation of a prebiotic hydrothermal alkaline scenario combining a highly reactive mineral surface, such as pyrite, and an extensive prebiotic reactant, such as cyanide, surprisingly led to the generation of a film that could protect against oxidation over the pyrite surface under wet conditions, and this film was

immediately effective. The quantification of the oxidized species formed from the iron sulfide surface and the inalterability observed in the composition of the coatings over the period of time considered herein show that prebiotic chemistry inspires useful organic polymeric materials, in this particular case, for efficient and inexpensive protective corrosion coatings. In addition, the unexpected results shown here offer a new perspective about the role of the interaction of mineral surfaces with organics in prebiotic chemistry research.

Experimental

Cleaning and coating processes on the pyrite surface

Samples of pyrite (from the Navajun mine in Spain) were cleaned three times in different solutions of 1 M H_2SO_4, immersed in water (Milli-Q grade) and then dried by blowing compressed air.

The cleaned pyrite samples were coated by direct immersion in equimolar aqueous solutions (10 mL) of NaCN and NH_4Cl (1 M) under ambient conditions (air conditions as described in the main text) or under an inert atmosphere of nitrogen (anoxic conditions). The reactions were performed in 20 mL glass vials fitted with Teflon/silicone septa and placed into metal heating blocks at 80 °C for 40 min. For synthesis under anoxic conditions, the system was successively evacuated with a pump and purged with nitrogen for 4 times, and double-distilled (dd) water was bubbled with dried N_2 for 20 min to remove the residual traces of oxygen. When the desired time was reached, the reaction mixture was immediately cooled. The coated samples were washed several times with dd water until colourless solutions were obtained and then dried by blowing compressed air. NaCN and NH_4Cl reagents were supplied by Panreac Química S.A.

Finally, the pyrite samples were transferred to an ultrahigh vacuum (UHV) chamber with a base pressure of 1×10^{-9} mbar to perform X-ray photoelectron spectroscopy (XPS) measurements. In the cases where it was required to store the pyrite samples overnight prior to running the XPS measurement the following day, the sample was kept under vacuum conditions to avoid sample degradation or contamination.

XPS spectroscopy analysis

X-ray photoelectron spectroscopy analysis of the samples was carried out in an ultrahigh vacuum chamber equipped with a hemispherical electron analyser and with the use of an Al Kα X-ray source (1486.6 eV) with an aperture of 7 mm × 20 mm. The base pressure in the chamber was 1×10^{-9} mbar, and the experiments were performed at room temperature. The XPS data were analysed using Fitt 1.2 software. The core level peak regions were deconvoluted into different components as a convolution of Gaussian and Lorentzian curves. The background was subtracted before the deconvolution analysis. The binding energy of the C 1s peak at 285.0 eV was used for calibration of the spectral data. The intensity ratio of the N to C peaks, normalized to their respective cross-sections, was proportional to the NH_4CN-based film formed on the pyrite surface.

The thickness of the NH_4CN-based organic layer was calculated from the Fe $2p_{3/2}$ peak intensities on a clean pyrite sample and pyrite after polymer adsorption under inert and air conditions based on the assumption that the attenuation length obeys the equation given by Whitesides *et al.*[39] These values of the thickness of the NH_4CN-based polymer layer under inert and air conditions were estimated to be 15 Å and 65 Å, respectively, which confirm successful polymer adsorption in both cases.

Author contributions

E. Mateo-Marti and M. Ruiz-Bermejo conceived, designed and supervised the project. E. M. M, M. R. B, S. G. M. and C. P. F. performed the experiments. S. G. M. and C. P. F performed the XPS measurements. E. M. M, S. G. M. and C. P. F analysed the XPS data. E. M. M and M. R. B wrote and revised the manuscript.

Conflicts of interest

There are no conflicts to declare.

Acknowledgements

The authors used the research facilities of the Centro de Astrobiología (CAB) and were supported by the Instituto Nacional de Técnica Aeroespacial "Esteban Terradas" (INTA), by the projects PID2019-104205GB-C21 and PID2019-107442RB-C32 from the Spanish Ministerio de Ciencia, Innovación y Universidades and by the Spanish State Research Agency (AEI) project MDM-2017-0737 Centro de Astrobiología (CSIC-INTA), Unidad de Excelencia María de Maeztu. We acknowledge S. Martín and B. Martín for cutting and polishing the pyrite samples and Thomas and Celine Huttel Serrano for providing them.

Notes and references

1 M. Ruiz-Bermejo, M.-P. Zorzano and S. Osuna-Esteban, *Life*, 2013, **3**, 421–448.
2 C. N. Matthews and R. D. Minard, *Faraday Discuss.*, 2006, **133**, 393–401.
3 T. Das, S. Ghule and K. Vanka, *ACS Cent. Sci.*, 2019, **5**, 1532–1540.
4 J. D. Toner and D. C. Catling, *Geochim. Cosmochim. Acta*, 2019, **260**, 124–132.
5 R. A. Sanchez, J. P. Ferris and L. E. Orgel, *J. Mol. Biol.*, 1967, **30**, 223–253.
6 J. D. Sutherland, *Angew. Chem., Int. Ed.*, 2016, **55**, 104–121.
7 M. d'Ischia, P. Manini, M. Moracci, R. Saladino, V. Ball, H. Thissen, R. A. Evans, C. Puzzarini and V. Barone, *Int. J. Mol. Sci.*, 2019, **20**, 4079.
8 H. Thissen, A. Koegler, M. Salwiczek, C. D. Easton, Y. Qu, T. Lithgow and R. A. Evans, *NPG Asia Mater.*, 2015, **7**, e225.

9 D. J. Menzies, A. Ang, H. Thissen and R. A. Evans, *ACS Biomater. Sci. Eng.*, 2017, **3**, 793–806.
10 J. Jung, D. J. Menzies, H. Thissen, C. D. Easton, R. A. Evans, R. Henry, A. Deletic and D. T. McCarthy, *J. Hazard. Mater.*, 2019, **378**, 120749.
11 W.-H. Chen, T.-Y. Liao, H. Thissen and W.-B. Tsai, *ACS Biomater. Sci. Eng.*, 2019, **5**, 6454, DOI: 10.1021/acsbiomaterials.9b00871.
12 T.-Y. Liao, C. D. Easton, H. Thissen and W.-B. Tsai, *ACS Biomater. Sci. Eng.*, 2020, **6**, 3349–3360.
13 H. Thissen, R. A. Evans and V. Ball, *Processes*, 2021, **9**, 82.
14 V. Ball, *Mater. Lett.*, 2021, **285**, 129050.
15 M. Ruiz-Bermejo, J. L. de la Fuente, J. Carretero-González, L. García-Fernández and M. R. Aguilar, *Chem.–Eur. J.*, 2019, **25**, 11437–11455.
16 X. Zhou, Y. Fang, Y. Su, C. Ge, B. Jin, Z. Li and S. Wu, *Catal. Commun.*, 2014, **46**, 197–200.
17 M. Rahm, J. I. Lunine, D. A. Usher and D. Shalloway, *Proc. Natl. Acad. Sci. U. S. A.*, 2016, **113**, 8121–8126.
18 E. Schwartz, M. Koepf, H. J. Kitto, R. J. M. Nolte and A. E. Rowan, *Polym. Chem.*, 2011, **2**, 33–47.
19 C. Yang, B. Wang, L. Zhang, L. Yin and X. Wang, *Angew. Chem., Int. Ed.*, 2017, **56**, 6627–6631.
20 I. Mas, J. L. de la Fuente and M. Ruiz-Bermejo, *Eur. Polym. J.*, 2020, **132**, 109719.
21 R. J. Toh, R. Evans, H. Thissen, N. H. Voelcker, M. d'Ischia and V. Ball, *Langmuir*, 2019, **35**, 9896–9903.
22 I. Mas, C. Hortelano, M. Ruiz-Bermejo and J. L. de la Fuente, *Eur. Polym. J.*, 2021, **143**, 110185.
23 G. Wächtershäuser, *Chem. Biodiversity*, 2007, **4**, 584–602.
24 K. M. Rosso, U. Becker and M. F. Hochella, *Am. Mineral.*, 1999, **84**, 1535–1548.
25 M. Sanchez-Arenillas and E. Mateo-Marti, *Phys. Chem. Chem. Phys.*, 2016, **18**, 27219–27225.
26 E. Mateo-Martí, C. Briones, C. Rogero, C. Gomez-Navarro, Ch. Methivier, C. M. Pradier and J. A. Martín-Gago, *Chem. Phys.*, 2008, **352**, 11–18.
27 E. Mateo-Marti, S. Galvez-Martinez, C. Gil-Lozano and M.-P. Zorzano, *Sci. Rep.*, 2019, **9**, 15311.
28 C. Mompeán, M. R. Marín-Yaseli, P. Espigares, E. González-Toril, M.-P. Zorzano and M. Ruiz-Bermejo, *Sci. Rep.*, 2019, **9**, 1916.
29 P. B. Rimmer and O. Shorttle, *Life*, 2019, **9**, 12.
30 M. Labadie, R. Jensen and E. Neuzil, *Biochim. Biophys. Acta, Gen. Subj.*, 1968, **165**, 525–533.
31 J. P. Ferris, E. H. Edelson, N. M. Mount and A. E. Sullivan, *J. Mol. Evol.*, 1979, **13**, 317–330.
32 J. P. Ferris, W. J. Hagan, K. W. Alwis and J. McCrea, *J. Mol. Evol.*, 1982, **18**, 304–309.
33 A. Negrón-Mendoza, S. Ramos-Bernal, E. Cruz and J. M. Juárez, *Radiat. Phys. Chem.*, 2001, **61**, 771–772.
34 J. W. Boclair, P. S. Braterman, B. D. Brister, J. Jiang, S. Lou, Z. Wang and F. Yarberry, *Origins Life Evol. Biospheres*, 2001, **31**, 53–69.
35 M. Colín-García, A. Heredia, A. Negrón-Mendoza, F. Ortega, T. Pi and S. Ramos-Bernal, *Int. J. Astrobiol.*, 2014, **13**, 310–318.
36 A. Fernández, M. Ruiz-Bermejo and J. L. de la Fuente, *Phys. Chem. Chem. Phys.*, 2018, **20**, 17353–17366.
37 M. Ruiz-Bermejo, J. L. de la Fuente and M. R. Marín-Yaseli, *J. Anal. Appl. Pyrolysis*, 2017, **124**, 103–112.
38 S. W. Knipe, J. R. Mycroft, A. R. Pratt, H. W. Nesbitt and G. M. Bancroff, *Geochim. Cosmochim. Acta*, 1995, **59**, 1079–1090.
39 P. E. Laibinis, C. D. Bain and G. M. Whitesides, *J. Phys. Chem.*, 1991, **95**, 7017–7021.